The accuracy with which (1) describes the actual output can be determined by comparing it with the solution obtained by using the exact transfer function of the waveguide. It is believed that this solution has not as yet been obtained in a closed form. However, some work for the case of a step function carrier utilizing numerical integration of the exact transfer function of the waveguide has been performed for a few specific cases.[8]

It is interesting to compare the waveforms predicted from this work with those utilizing the approximate transfer function given by (15). For a step function input of

$$e(t) = E_0 \sin \omega_0 t \; 1(t), \tag{19}$$

where $1(t)$ is the step function defined by

$$1(t) = \begin{cases} 1 & t > 0 \\ 0 & t < 0, \end{cases} \tag{20}$$

the output of a waveguide characterized by the approximate transfer function of (15), via (18) or following Elliott, is

$$f(t) = \frac{E_0}{2} \exp \{ j[\omega_0 t - \beta_0 L] \} \operatorname{erfc} Z_0, \tag{21}$$

where it is understood that the imaginary part of (21) is to be taken for $f(t)$, and with

$$Z_0 = -\frac{(t - AL)(1 + j)}{2\sqrt{2BL}}, \tag{22}$$

where

$$\operatorname{erfc} Z_0 = \frac{2}{\sqrt{\pi}} \int_{Z_0}^{\infty} e^{-z^2} dz. \tag{23}$$

Integration of (23) gives for the output envelope $F(t)$

$$F(t) = |f(t)| = \frac{E_0}{2} \cdot \sqrt{1 + 2[C^2(A_1') + S^2(A_1') + C(A_1') + S(A_1')]}. \tag{24}$$

where A_1' is given by (13) and $C(A)$ and $S(A)$ by (4) and (5), respectively.

Plots of $F(t)$ via (24) (which is essentially based on Elliott's work), and of $F(t)$ (based on the work and Figs. 3 and 4 of Cohn[8]) are shown in Fig. 2. These plots are for the two cases

$$\frac{\omega_0}{\omega_c} = 1.10, \qquad \frac{L}{\lambda_{v0}} = 0.875$$

and

$$\frac{\omega_0}{\omega_c} = 1.10, \qquad \frac{L}{\lambda_{v0}} = 1.750,$$

where λ_{v0} = vacuum wavelength of excitation $= c/f_0$, $f_0 = \omega_0/2\pi$, c = speed of light.

The work of Cohn indicates that the output pulse starts at the time L/c, not L/v_g, where

$$v_g = \text{group velocity} = \frac{1}{A} = \left(\frac{d\beta}{d\omega}\bigg|_{\omega=\omega_0} \right)^{-1} = \frac{c\left[\left(\frac{\omega_0}{\omega_c}\right)^2 - 1\right]^{1/2}}{\left(\frac{\omega_0}{\omega_c}\right)}.$$

[8] G. I. Cohn, "Electromagnetic transients in Waveguides," *Proc. NEC*, Chicago, Ill., September 29–October 1, 1952, vol. 8, pp. 284–295.

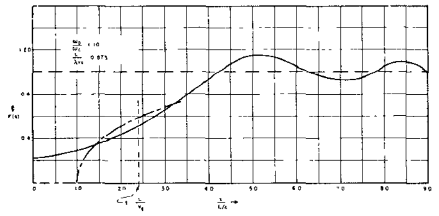

(a)

– – – steady state envelope
——— $F(t) = (1/2)\sqrt{1+2(C^2A_1'+S^2A_1'+CA_1'+SA_1')}$ (via approximate transfer function)
— — — $F(t)$ via exact transfer function and numerical integration (Reference 8 Fig. 3)

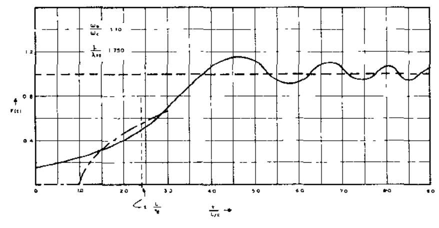

(b)

– – – – steady state envelope
——— $F(t) = (1/2)\sqrt{1+2(C^2A_1'+S^2A_1'+CA_1'+SA_1')}$ (via approximate transfer function)
- - - - - $F(t)$ via exact transfer function and numerical integration (Reference 8 Fig. 4)

Fig 2—Output waveform of a waveguide due to a step function carrier input.

For the case of Fig. 2, $c/v_g = 2.40$. This is in accordance with the meaning of wave front velocity.[9] The plots of Fig. 2 indicate that the waveform envelope predicted using the approximate transfer function of the waveguide given by (15) approximates that obtained via numerical integration, using the exact transfer function of the waveguide quite well for the time range indicated. The envelope for $t < 0$ via the approximate transfer function is not shown but is nonzero. The close agreement for this step function input for the specific cases of ω_0/ω_c and L/λ_{v0} indicate that the use of the approximate transfer functions gives a good approximation for the output waveform for the time ranges available for comparison. Generalizing from this comparison, one would expect the same approximation to be as good for the pulsed carrier input and hence that for $t > L/c$ that the envelope shapes of Fig. 1 are good approximations to the output pulse shapes of a waveguide. It would be in order, however, to confirm this generalization by obtaining an exact closed form solution for the pulsed case.

Acknowledgment

The authors are obliged to H. Hodara and R. Jacobson of The Hallicrafters Company for technical discussion and computational assistance, respectively.

C. M. Knop
The Hallicrafters Co.
Chicago, Ill.
G. I. Cohn
NESCO
Pasadena, Calif.

[9] J. A Stratton, "Electromagnetic Theory," McGraw-Hill Book Co., Inc., New York, N. Y., p. 337; 1941.

Temperature Stabilization of Gyromagnetic Couplers*

A gyromagnetic coupler using a single-crystal YIG sphere as a coupling element suffers from two significant sources of temperature instability. One of these is anisotropy drift,[1] a characteristic that is internal to the coupling element, since it stems directly from temperature induced variations in crystalline anisotropy.[2] The other is appropriately characterized as external; it derives from temperature induced variations in the magnetic biasing source. Either or both of these variations will result in a change in the resonant frequency of a gyromagnetic coupler. The 3-db bandwidth of a low loss YIG coupler may be of the order of 40 Mc, hence a change in resonant frequency of as little as 5 Mc will be detected as an increase in insertion loss at the original frequency. It is therefore quite desirable that the variations which contribute to this instability be reduced to a minimum. Means have been developed for eliminating both of these instabilities, thus rendering the gyromagnetic coupler a much more practical device under a variety of environmental conditions.

For power limiting applications at relatively high power levels, such as those previously reported by the authors at *C*-band frequencies,[3,4] a problem arises through high power heating of the YIG crystal. Under some conditions the resultant anisotropy drift can have an appreciable effect on the operation of the device. The authors observed this effect in a test arrangement in which a high power pulse of variable amplitude is closely followed by a low power pulse ($\approx$1 mw) of constant amplitude. With the YIG crystal (23 mils in diameter) randomly oriented and a constant dc magnetic field applied, a drift in the frequency of optimum transmission for the low power signal of more than 40 Mc has been observed when the high power signal is raised from 0 to 1000-w peak, 1-w average.

Crystalline orientation is the direct solution to the problem of anisotropy drift. With the biasing field restricted to a 110 plane, profitable use can be made of the equation[5]

$$H_{\text{eff}}^2 = (H_0 + AH_a)(H_0 + BH_a)$$

where second-order anisotropy effects are neglected and spherical geometry is assumed.

* Received October 3, 1962; revised manuscript received May 16, 1963. This work was supported in part by the Bureau of Naval Weapons, and in part by the Microwave Tubes Branch, U. S. Army Signal Research and Development Labs. under Contract DA-36-039-SC-85330.

[1] The problem of anisotropy drift in lithium ferrite single crystals in gyromagnetic couplers was discussed by S. Okwit at the 1962 PGMTT National Symposium.

[2] A. M Bozorth, "Ferromagnetism," D. Van Nostrand Company, Inc., Princeton, N. J.; 1951.

[3] J. Clark and J. Brown, "The gyromagnetic coupling limiter at *C*-band," IRE Trans. on Microwave Theory and Techniques (*Correspondence*), vol. MTT-10, pp 84–85, January, 1962.

[4] J Brown and J. Clark, "Practical microwave power limiters," IRE Trans. on Microwave Theory and Techniques (*Correspondence*), vol. MTT-10, pp. 85–86; January, 1962.

[5] P. J. B Clarricoats, "Microwave Ferrites," John Wiley and Sons, Inc., New York, N. Y., 1961.

H_0 = the applied field,
$H_a = K_1/4\pi M_s \approx 30$ oersteds for YIG,
$A = 2 - \sin^2\theta - 3\sin^2 2\theta$
$B = 2(1 - 2\sin^2\theta - \frac{3}{8}\sin^2 2\theta)$,
θ = angle between 100 axis and the applied field with the applied field in a 110 plane.

Expanding:

$$H_{\text{eff}}^2 = H_0^2 + AH_0H_a + BH_0H_a + ABH_a^2.$$

For a YIG sphere at C-band,

$$\frac{H_a^2}{H_0H_a} = \frac{H_a}{H_0} = \frac{30}{1500} = \frac{1}{50}.$$

The H_a^2 term is small and can be neglected for practical purposes.

$$H_{\text{eff}}^2 = H_0^2 + (A + B)H_0H_a.$$

The desired temperature stable condition occurs when $A + B = 0$.

A solution for θ under these conditions yields $\theta = 29°40'$ for the angle between the biasing field and the 100 axis, at which anisotropy effects contribute the least to the effective field for resonance. Hopefully, this contribution will be small enough that a relatively large anisotropy drift with temperature will cause negligible shift in this effective field; thus the problem of anisotropy drift in a gyromagnetic coupler could be circumvented with the YIG sphere properly oriented in the device.

In order to check these calculations the authors devised the test structure of Fig. 1. An expanded sketch of the sphere mounting is shown in Fig. 2. This structure is designed to be operated between the poles of an electromagnet with the biasing field applied as indicated. The garnet crystal is prealigned on the dielectric rod in such a manner that the biasing field remains in an 110 plane as the rod is rotated around its long axis; and the rod is so positioned in the device that the crystal serves as a coupling element between the orthogonal lines. A small bifilar wound heating element is placed in proximity to the crystal and a thermocouple is included nearby.

With this arrangement, it is possible to measure the field required for optimum microwave transmission through the device, which corresponds with the field required for resonance, as a function of both angular position and temperature. The angular orientation requiring the maximum field for resonance at a given temperature locates a hard direction, corresponding to a 100 axis. With this direction taken as a zero reference for angular measurement at each temperature, the data of Fig. 3 were obtained. As expected, the effect of anisotropy drift on the effective field for resonance is a minimum at an angle of about 30°.

A total of five single crystal YIG spheres, all approximately 23 mils in diameter with $\Delta H < 0.5$ oe, were X-ray aligned within 1° of this angle. The Laue back reflection pattern to be obtained is illustrated in Fig. 4. These spheres were transferred into a gyromagnetic coupling structure which is useful as a power limiter at peak powers in excess of 5 kw. The accuracy of alignment maintained during the transfer is difficult to assess; for this reason the accuracy of final alignment within the device should perhaps not be claimed to less than 3 or 4 degrees.

Anisotropy drift was checked with the two-pulse technique described earlier. The high power signal was varied between zero and 5-kw peak, 5 watts average. The maximum observed drift in optimum frequency of transmission of the low power signal was approximately 10 Mc, and in one case no detectable drift was observed. These results were a substantial improvement over those obtained with randomly oriented samples.

In most cases anisotropy drift was not apparent below the level of about 1-kw peak, 1 w average. The problem of anisotropy drift was considered to be solved for gyromagnetic couplers operating below this power level, and it was assumed that the external sources of instability in these devices could now be regarded as an independent problem.

This problem is essentially one of temperature compensating the magnetic biasing source. The heart of the problem is the degree of compensation required. A well stabilized but uncompensated Alnico V magnet will have a temperature coefficient for field change in the neighborhood of 0.016 per cent/F°. In a gyromagnetic coupler at C band this translates into a drift in frequency of optimum transmission of roughly 1 Mc/F°. In a device with a 3-db bandwidth of from 20 to 40 Mc, this kind of drift quickly becomes troublesome. Field stability of a gauss or less is considered necessary for truly practical operation. Stated in more concrete terms, the problem becomes one of compensating the magnet to this degree over an extended temperature range and also over any tuning range that the coupler might be required to cover.

The solution to the problem of magnet compensation was surprisingly simple. A small strip of Carpenter Temperature Compensator[6] in parallel with the air gap of a C magnet was found sufficient to do the job over the required temperature range of −20°F to +150°F, and over the required coupler tuning range, from 5.4 to 5.7 Gc. No data are available on the compensation achieved in terms of gauss, since the coupler itself was used as the field sensing element, and the success of the compensator determined directly from the microwave behavior of the coupler as a function of temperature. The data thus obtained are illustrated in Fig. 5. In this connection it would be pointed out that the magnetic circuit to be compensated included, in addition to the Alnico V magnet, two soft iron pole peaces, a soft iron sheet metal shield of $\frac{1}{8}$ inch wall thickness entirely surrounding the device, and an independent slug of soft iron used as a magnetic shunt for tuning the

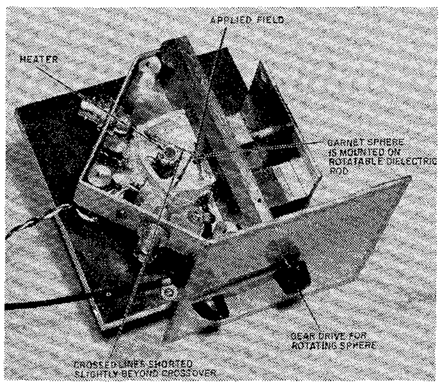

Fig. 1—Test structure for the measurement of anisotropy drift as a function of temperature and orientation.

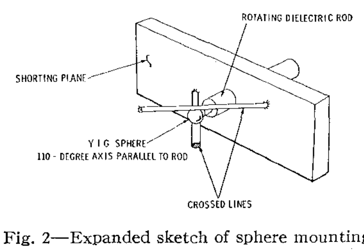

Fig. 2—Expanded sketch of sphere mounting.

[6] Information on Carpenter Temperature Compensator can be obtained directly from The Carpenter Steel Company, Reading, Pa.

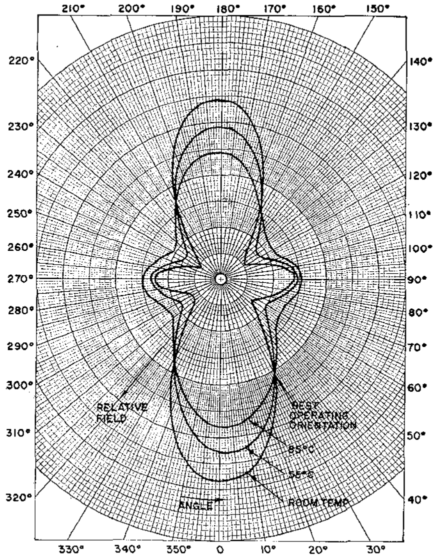

Fig. 3—Applied field for resonance as a function of temperature and angle (applied field in a 110 plane).

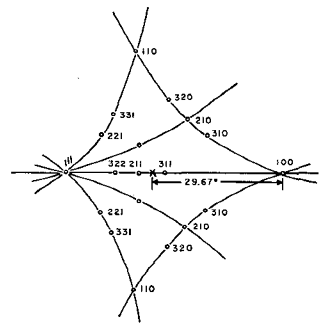

Fig. 4—The Laue back reflection pattern of the temperature stable orientation.

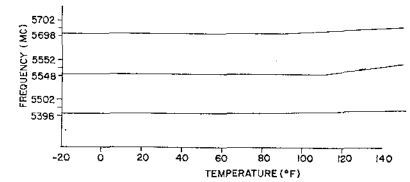

Fig. 5—Frequency of optimum transmission vs temperature for a temperature stabilized gyromagnetic coupler at C-band.

center frequency of the coupler. The exact role that each of these elements plays in the final, fully compensated configuration is difficult to assess, and no attempt at a detailed analysis has been made.

In summary, a solution to the problem of anisotropy drift in a YIG single crystal gyromagnetic coupler has been achieved through the appropriate orientation of the YIG coupling element. A solution to the external source of instability has been achieved through the use of a magnetic shunt of Carpenter Temperature Compensator. The end product is a well shielded gyromagnetic coupler, tunable from 5.4 to 5.7 Gc, free from anisotropy drift affects with up to 1 watt average power input, and temperature stabilized to less than ±2 Mc through an ambient change from −20°F to 150°F.

ACKNOWLEDGMENT

The authors wish to thank Drs. G. P. Rodrigue and J. E. Pippin of Sperry Microwave Electronics Company, Research Section, for many valuable suggestions.

J. CLARK
J. BROWN
D. E. TRIBBY
Advance Microwave Techniques Dept.
Sperry Microwave Electronics Co.
Clearwater, Fla.

An S-Band Wide-Band Degenerate Parametric Amplifier*

This communication reports some experimental results for an S-band wide-band degenerate parametric amplifier designed with a method earlier described by the author.[1]

We represent the varactor by a nonlinear capacitance in series with a loss resistance R and an inductance L_s and write the pumped capacitance as

$$C = C_d[1 + 2\alpha \cos \omega_p t]. \tag{1}$$

Then the signal voltage gain G of a degenerate circulator operated amplifier can be written as

$$\begin{cases} |G| = \dfrac{1 + |\rho|^2}{2|\rho|} \\ \rho = \dfrac{Z_s - Z_d}{Z_s + Z_d} \end{cases}. \tag{2}$$

Z_s is the signal circuit impedance, including varactor reactances, as seen from the varactor end. Z_d is a modified signal-idler coupling impedance

$$\begin{cases} Z_{d0} = \dfrac{\alpha}{\omega_{s0}(1 - \alpha^2)C_d} \\ Z_d = \sqrt{Z_{d0}^2 + \dfrac{R^2}{G_0^2 - 1}} - R\dfrac{G_0}{\sqrt{G_0^2 - 1}} \end{cases}. \tag{3}$$

* Received May 24, 1963.

[1] B. T. Henoch, "A new method for designing wide-band parametric amplifiers," IEEE TRANS. ON MICROWAVE THEORY AND TECHNIQUES, vol. MTT-11, pp. 62–72; January, 1963.

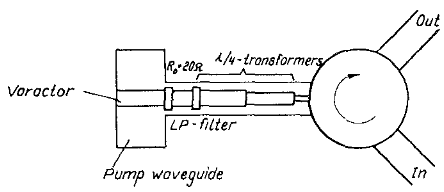

Fig. 1—Configuration of a single-tuned amplifier.

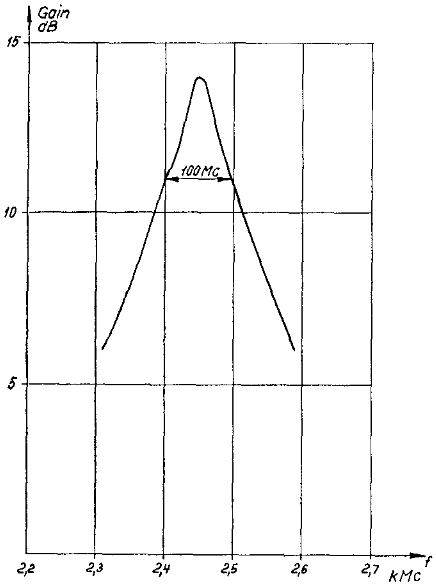

Fig. 2—Double sideband gain as a function of frequency for the single-tuned amplifier.

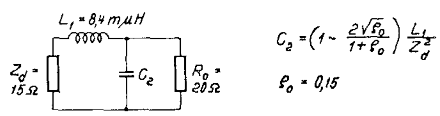

Fig. 3—Low-pass equivalent of the matching circuit.

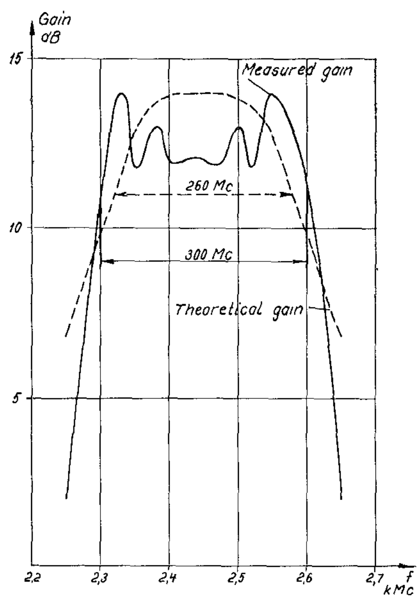

Fig. 4—Double sideband gain as a function of frequency for the double-tuned amplifier.

The wide-band design problem now is reduced to a problem of matching the modified coupling impedance Z_d into the amplifier source impedance R_0.

The experimental amplifier uses a GaAs varactor with a zero-bias capacitance of 0.5 pf, cutoff frequency 100 kMc and series-resonance frequency 6 kMc. The varactor is mounted in a pump waveguide according to Fig. 1.

The signal frequency is chosen so that the waveguide inductance resonates the varactor and the amplifier source impedance R_0 is chosen to 20 Ω.

The double sideband gain is measured by using a swept frequency generator and a broad-band detector which displays the gain curve on an oscilloscope. The gain vs frequency for the single-tuned amplifier is shown in Fig. 2.

The measured gain curve corresponds to $C_d = 0.5$ pf, $Z_d = 15$ Ω and $\alpha = 0.15$. The inductance L_1 in the series resonator is $L_1 = 8.4$ mμh.

To get a double-tuned wide-band amplifier a parallel resonator is inserted between the series-tuned varactor and the amplifier source impedance R_0 and designed to match Z_d maximally flat into R_0. The low-pass equivalent of the matching circuit is shown in Fig. 3.

Practically, a low impedance section, half a wavelength long at ω_{s0}, is used as a parallel resonator. From a linear approximation around ω_{s0} the impedance Z_p of the low impedance section can be determined.

$$C_2 = \frac{1}{2}\frac{\pi}{\omega_{s0}}\left[\frac{1}{Z_p} - \frac{Z_p}{R_0^2}\right]. \tag{4}$$

This determines Z_p to 7 Ω. Plotting in a Smith Chart shows that the optimum Z_p will be somewhat lower than given by (4). Reactive parts in the source impedance R_0 might modify the length of the low impedance section.

With a low impedance section of impedance 5.5 Ω and electrical length 170° at ω_{s0} the gain curve shown in Fig. 4 is measured. The measured gain curve is compared with a theoretical gain curve obtained from the concentrated element equivalent.

Point measurements of the double sideband noise figure give noise figures of 1.5–2.0 db.

BENGT T. HENOCH
Research Institute of National Defence
Stockholm, Sweden

Phaseshift of Electromagnetic Waves Propagating Through Waveguide Junctions*

This work was activated by the lack of information in literature about the effect of an H-plane branch upon electromagnetic waves traveling through the collinear arms of the branch. Most literature about the sub-

* Received March 29, 1963; revised manuscript received April 29, 1963.